Woo Je Lee,[1,2] Sanshiro Tateya,[1,2] Andrew M. Cheng,[1,2] Norma Rizzo-DeLeon,[1,2] Nicholas F. Wang,[1,2] Priya Handa,[1,2] Carole L. Wilson,[3] Alexander W. Clowes,[4] Ian R. Sweet,[1,2] Karol Bomsztyk,[1] Michael W. Schwartz,[1,2] and Francis Kim[1,2]

M2 Macrophage Polarization Mediates Anti-inflammatory Effects of Endothelial Nitric Oxide Signaling

Diabetes 2015;64:2836–2846 | DOI: 10.2337/db14-1668

Endothelial nitric oxide (NO) signaling plays a physiological role in limiting obesity-associated insulin resistance and inflammation. This study was undertaken to investigate whether this NO effect involves polarization of macrophages toward an anti-inflammatory M2 phenotype. Mice with transgenic endothelial NO synthase overexpression were protected against high-fat diet (HFD)-induced hepatic inflammation and insulin resistance, and this effect was associated with reduced proinflammatory M1 and increased anti-inflammatory M2 activation of Kupffer cells. In cell culture studies, exposure of macrophages to endothelial NO similarly reduced inflammatory (M1) and increased anti-inflammatory (M2) gene expression. Similar effects were induced by macrophage overexpression of vasodilator-stimulated phosphoprotein (VASP), a key downstream mediator of intracellular NO signaling. Conversely, VASP deficiency induced proinflammatory M1 macrophage activation, and the transplantation of bone marrow from VASP-deficient donor mice into normal recipients caused hepatic inflammation and insulin resistance resembling that induced in normal mice by consumption of an HFD. These data suggest that proinflammatory macrophage M1 activation and macrophage-mediated inflammation are tonically inhibited by NO → VASP signal transduction, and that reduced NO → VASP signaling is involved in the effect of HFD feeding to induce M1 activation of Kupffer cells and associated hepatic inflammation. Our data implicate endothelial NO → VASP signaling as a physiological determinant of macrophage polarization and show that signaling via this pathway is required to prevent hepatic inflammation and insulin resistance.

In addition to their primary role in host defense, macrophages participate in a variety of homeostatic functions, including wound healing and tissue repair (1–3). These pleiotropic effects are mediated by the macrophage response to diverse environmental signals that give rise to distinct functional phenotypes that can range from proinflammatory (classic M1 activation) to a more anti-inflammatory phenotype (alternative M2 activation) that promotes tissue repair (4,5). In response to interferon (IFN)-γ and Toll-like receptor ligands, such as lipopolysaccharide (LPS), for example, macrophages adopt an M1 phenotype that is characterized by the expression of a variety of proinflammatory genes. In contrast, the M2 phenotype, which can promote the resolution of inflammation, is adopted by macrophages in response to exposure to interleukin (IL)-4 and IL-13. Although some nuclear receptors, transcription factors, and coactivators have been identified as regulators of macrophage phenotype responses (6,7), the molecular mechanisms governing macrophage polarization remain incompletely characterized.

Accumulating evidence supports a role for tissue macrophages in a broad spectrum of inflammatory conditions (8), including obesity-associated metabolic diseases such as insulin resistance and type 2 diabetes (9,10). Low-grade inflammation in this setting is mediated in part by the polarization of recruited and resident macrophages to the M1 phenotype in tissues such as liver and adipose tissue (11,12). In contrast, M2 macrophage activation appears to protect against obesity-associated inflammation and insulin resistance (13,14).

[1]Department of Medicine, University of Washington, Seattle, WA
[2]Diabetes and Obesity Center of Excellence, University of Washington, Seattle, WA
[3]Department of Pathology, University of Washington, Seattle, WA
[4]Department of Surgery, University of Washington, Seattle, WA

Corresponding author: Francis Kim, fkim@u.washington.edu.

Received 31 October 2014 and accepted 21 March 2015.

W.J.L. is currently affiliated with the Department of Medicine, ASAN Medical Center, University of Ulsan College of Medicine, Seoul, Republic of Korea.

S.T. is currently affiliated with the Department of Medicine, Kobe University Graduate School of Medicine, Kobe, Japan.

See accompanying article, p. 2711.

Endothelial nitric oxide (NO) is a signaling molecule that is generated by the conversion of L-arginine to citrulline via the enzyme endothelial NO synthase (eNOS). In contrast to the proinflammatory effect of exposure to high NO levels, the low concentrations of NO produced by eNOS in the vessel wall mediate vasodilation and an assortment of anti-inflammatory, antithrombotic, and antiproliferative functions (15,16). The signal transduction pathway responsible for these effects involves activation by NO of soluble guanylate cyclase, which in turn activates cyclic guanosine monophosphate (cGMP)–dependent protein kinase (PKG) by increasing cytoplasmic cGMP levels. Among downstream targets of PKG is vasodilator-stimulated phosphoprotein (VASP), which has been implicated in the control of cell migration and cytoskeletal remodeling (17,18). That endothelial NO/VASP signaling exerts anti-inflammatory effects in vivo is suggested by evidence of hepatic and adipose tissue inflammation and insulin resistance—resembling the response to high-fat diet (HFD) feeding—in mice lacking either eNOS or VASP (19,20). Moreover, these effects are associated with M1 activation of Kupffer cells, the resident macrophage of the liver (19). Together with the observation that HFD-induced obesity reduces endothelial NO signaling in these tissues (21), we proposed the following three-part hypothesis: *1*) NO/VASP signaling is a key regulator of macrophage polarization; *2*) in the liver, Kupffer cell M1 activation results from an obesity-associated decline of hepatic endothelial NO signaling; and *3*) this sequence is at least in part responsible for the effect of HFD feeding in inducing hepatic inflammation and insulin resistance. Our findings offer direct support for this hypothesis and thereby identify the endothelial NO/VASP signaling pathway as a novel regulator of macrophage polarization.

RESEARCH DESIGN AND METHODS

Animal Experiments

eNOS transgenic (*eNos Tg*) mice (22), provided by Dr. K. Hirata (Kobe University, Kobe, Japan), express bovine eNOS under the control of the preproendothelin-1 promoter (22) and were maintained on a C57BL/6 background. VASP knockout ($Vasp^{-/-}$) mice were also bred onto the C57BL/6 background (23). At 8 weeks of age, groups of male wild-type (WT) littermate controls (n = 20) and *eNos Tg* mice (n = 20) were placed on either a low-fat diet (LFD) (10% fat; catalog #D12450B; Research Diets, New Brunswick, NJ) or an HFD (60% of calories from fat; catalog #D12492; Research Diets) and maintained for indicated periods. BH4 (6R-5,6,7,8-tetrahydro-L-biopterin dichloride) is an important eNOS cofactor that is readily oxidized in animals with obesity or diabetes, resulting in reduced BH4 levels (24–26). Decreased BH4 levels can in turn uncouple eNOS, thereby increasing the production of superoxide while decreasing NO bioavailability in the liver (27). In the setting of BH4 deficiency, therefore, high eNOS levels generated by transgenic overexpression can be harmful. Consequently, BH4 (Enzo Life Sciences, Plymouth Meeting, PA) was added to both the LFD and HFD (0.3 mg/day). $Vasp^{-/-}$ mice (n = 10) and their littermate controls (n = 10) were maintained on an LFD for 4 weeks. Body weight and food intake were measured weekly.

For experiments using IL-4 in vivo, IL-4 complexes were prepared by mixing IL-4 and anti–IL-4 antibodies, and mice received daily intraperitoneal injections for 3 days prior to being killed, as previously described (28). Whole-body insulin signaling was assessed following insulin injection (0.06 units/g body wt i.p.) after an overnight fast. Fifteen minutes after insulin injection, mice were killed using an overdose of CO_2 followed by cervical dislocation. In all experiments, mice were maintained in a temperature-controlled facility with a 12-h light-dark cycle. All procedures were performed according to the National Institutes of Health *Guide for the Care and Use of Laboratory Animals* and were approved by the University of Washington Institutional Animal Care and Use Committee.

Materials

Anti–phosphorylation (p) inhibitor of B (IκB)-α, anti-PKG, anti-VASP, and anti–p-VASP (Ser 239), anti-Arginase1, anti-STAT6, anti–p-STAT6 (Tyr 641), and β-actin antibodies were from Cell Signaling Technology (Beverly, MA). Anti-eNOS mouse polyclonal antibody was obtained from BD Biosciences (Lexington, KY). Anti-GAPDH rabbit polyclonal antibody was obtained from Santa Cruz Biotechnology (Santa Cruz, CA). Biosource total Akt and p-Akt (Ser 473) ELISA kits were purchased from Invitrogen (Carlsbad, CA), and IRS2 and p-IRS2 ELISA kits were purchased from Cell Signaling Technology. Lactate was measured using an Amplex Red Glucose/Glucose Oxidase Assay Kit (Invitrogen). (Z)-1-[*N*-(2-aminoethyl)-*N*-(2-ammonioethyl)amino] diazen-1-IM1,2-diolate (DETA-NO) was purchased from Enzo Life Sciences. DETA-NO was used within 24 h after the reconstitution.

Quantitative RT-PCR Analyses

RNA was extracted using an RNase kit (Qiagen, Valencia, CA). For gene expression analysis, real-time RT-PCR reactions were conducted as described previously (21) using TaqMan Gene Expression Analysis (Applied Biosystems, Foster City, CA).

Western Blotting

Cell lysis and tissue extraction were performed as described previously (29). All Western blots used equal amounts of total protein for each condition from individual experiments and were performed as described previously (30).

Measurement of NO, Metabolic Parameters, and Hepatic Triglyceride Content

Tissue NO content was measured by using an electron spin resonance spectroscopy (ESR) technique, as previously described (21,31). Insulin levels were determined using a mouse insulin ELISA kit (Crystal Chem, Downers Grove, IL). Determinations of body lean and fat mass were made in conscious mice using quantitative magnetic resonance

(EchoMRI 3-in-1 body composition analyzer; Echo Medical Systems, Houston, TX) in the University of Washington Nutrition Obesity Research Center. Hepatic triglyceride (TG) content was enzymatically measured in liver lysates as previously described (32).

Insulin Tolerance Testing

Following an overnight fast, mice received an injection of insulin (0.75 units/kg body wt i.p.; Humulin R; Eli Lilly, Indianapolis, IN). Blood glucose was monitored (OneTouch Ultra; LifeScan) before and at serial time points after insulin administration.

Cell Culture

Bovine aortic endothelial cells (BAECs) were purchased from Cascade Biologics (Invitrogen); were cultured in RPMI 1640 medium supplemented with 10% FBS (HyClone Laboratories, Logan, UT), 12 μg/mL bovine brain extract (Lonza, Walkersville, MD), L-glutamine (2 mmol/L), sodium pyruvate (1 mmol/L), and nonessential amino acids in the presence of penicillin (100 units/mL) and streptomycin (100 μg/mL); and were maintained at 37°C in 5% CO_2. RAW macrophages were purchased from American Type Culture Collection and were cultured in DMEM (catalog #10–013-CV; Cellgro Mediatech, Manassas, VA) supplemented with 10% FBS in the presence of penicillin (100 units/mL) and streptomycin (100 μg/mL). Bone marrow–derived macrophages (BMDMs) were generated from mice, as described previously (33). For classic or alternative activation of macrophages, cells were stimulated with murine IFN-γ (12 ng/mL; STEMCELL Technologies, Vancouver, BC, Canada) plus LPS (5 ng/mL; Sigma-Aldrich, St. Louis, MO) for 24 h or with murine IL-4 (10 ng/mL; R&D Systems, Minneapolis, MN) for 48 h, respectively. A retroviral construct containing human WT VASP in the retroviral vector LXSN was used for overexpression studies. RAW cells were plated in six-well plates and allowed to grow for 24 h. The supernatant, containing either control LXSN or LXSN-wt-VASP virus, was mixed in HEPES and polybrene (8 μg/mL final concentration) and added to the RAW cells (23). Multiple clones were selected, propagated, and maintained in the presence of G418 (1 mg/mL; Cellgro Mediatech).

Kupffer Cell Isolation

Kupffer cells were isolated from liver tissue, as described previously (11) with minor modifications. After hepatic perfusion through the portal vein with Liver Digest Medium (Life Technologies) containing 0.05 mg/mL collagenase type 4 (Worthington Biochemical), the liver was minced with scissors for 20 min in a 60-mm dish and transferred into a 50-mL conical tube through a 70-mm cell strainer. After centrifugation (5 min at 50*g*), supernatants were collected and centrifuged for 10 min at 1,000*g*. The resultant pellets were resuspended with rat anti-F4/80 antibody (AbD Serotec), and magnetic beads were conjugated with sheep anti-rat IgG (Invitrogen) at 4°C for 30 min.

Coculture of Endothelial Cells and BMDMs

BMDMs were cultured in an insert on a semipermeable membrane (3401 Transwell; Corning) 24 h prior to the coculture with BAECs. BAECs were grown in the lower chamber and transfected with either negative control small interfering RNA (siRNA) (catalog #4390843; Ambion) or custom select siRNA for bovine eNOS (Ambion) using siPORT NeoFX Transfection Agent (Ambion) according to the manufacturer protocol. Sequences of siRNA for bovine eNOS are as follows: sense, 5′-GAGUUACAAGAUCCG CUUCTT-3′; antisense, 5′-GAAGCGGAUCUUGUAACUCTT 3′. BMDMs were placed into a well containing BAECs (BMDM/BAEC ratio 1:4) and cultured for 48 h.

Bone Marrow Transplant

Groups of male WT mice (C57BL/6), 6–8 weeks of age, were irradiated with a single dose of 9.7 Gy and subsequently transplanted via retro-orbital veins with marrow (7×10^6 cells) taken from the femur and tibia of either male WT mice (WT-BMT mice) or *Vasp*$^{-/-}$ mice (VASP KO-BMT mice). Treated mice were allowed to recover for 4 weeks on a standard chow diet and were then subsequently maintained on the LFD.

Statistical Analysis

In all experiments, densitometry measurements were normalized to controls incubated with vehicle, and the fold increase above the control condition was calculated. Analysis was performed using the STATA 8 statistical package. Data are expressed as the mean ± SEM, and P values of <0.05 were considered statistically significant. A two-tailed t test was used to compare mean values in two-group comparisons. For four-group comparisons, two-way ANOVA and the Bonferroni post hoc comparison test were used to compare mean values among the groups.

RESULTS

Effect of eNOS Overexpression on Whole-Body and Hepatic Responses to an HFD

Compared with LFD-fed WT controls, 8 weeks of HFD feeding caused obesity in both WT and *eNos Tg* mice (Fig. 1*A* and *B*), and since neither weight gain nor percent body fat differed between genotypes, transgenic eNOS overexpression did not appear to influence the obesity-inducing effect of HFD feeding in this study. Despite comparable obesity, the effect of diet-induced obesity to increase fasting insulin levels in HFD-fed WT mice was blunted in HFD-fed *eNos Tg* mice (Fig. 1*C*). Measurements of insulin tolerance (i.e., with an insulin tolerance test) (34) confirmed that during HFD feeding *eNos Tg* mice are much more insulin sensitive than WT control mice (Fig. 1*D*). In turn, the maintenance of normal hepatic NO levels during HFD feeding prevented the activation of hepatic nuclear factor-κB (NF-κB), a marker of inflammatory activation (Fig. 1*E* and *F*), and restored hepatic insulin signaling, as measured by insulin-stimulated phosphorylation of IRS2 and Akt (Fig. 1*G* and *H*). Hepatic steatosis is a common and pathophysiologically relevant complication of diet-induced

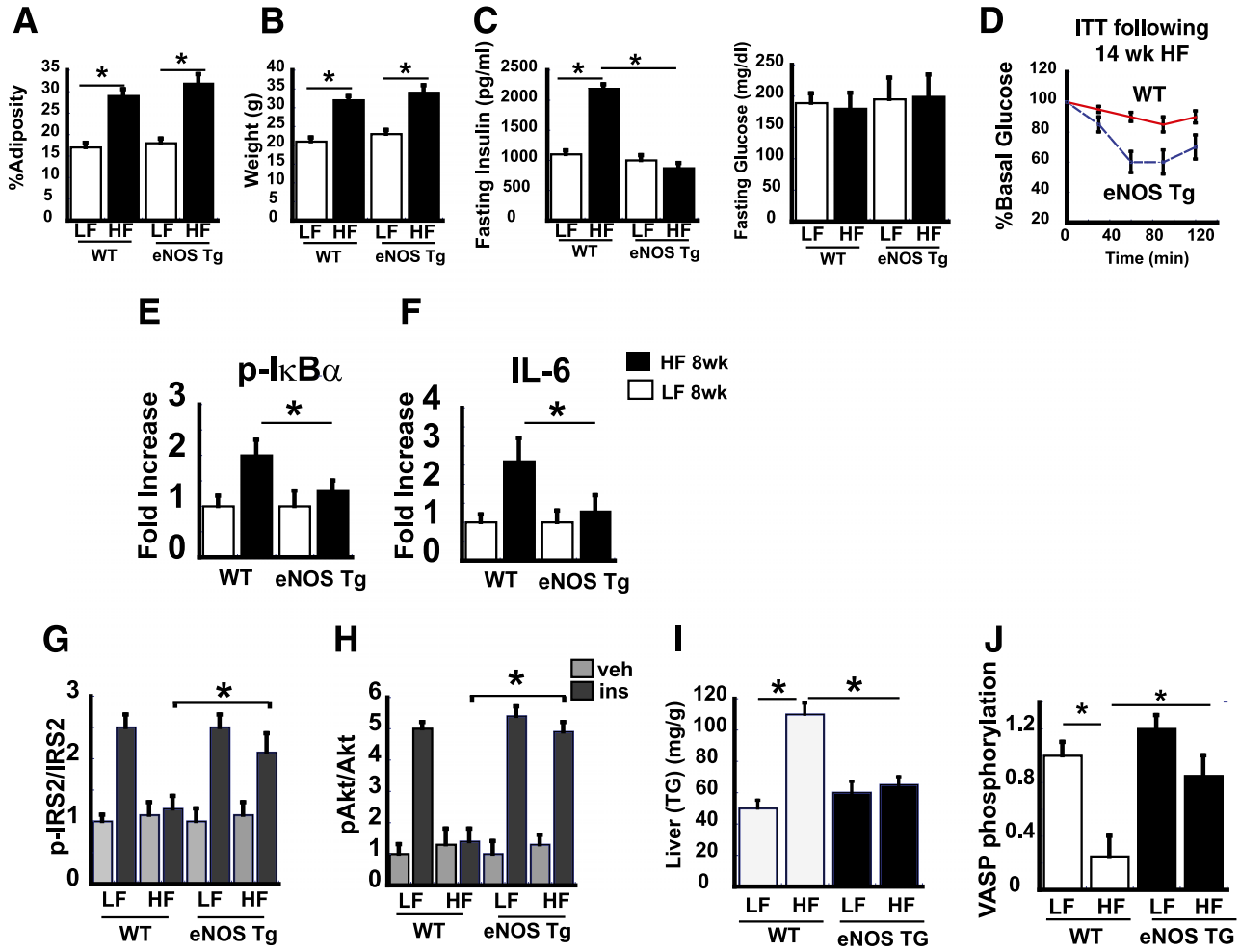

Figure 1—Effect of eNOS overexpression on whole-body and hepatic responses to an HFD (HF). WT control and *eNos Tg* mice, 8 weeks of age, were fed an LFD (LF) or an HFD for 8 (*A–C* and *E–J*) or 14 (*D*) weeks. Both LFD and HFD were supplemented with BH4. *A*: Adiposity (%) as measured by MRS. *B*: Body weight (g). *C*: Fasting serum insulin and glucose levels. *D*: After 14 weeks of being fed an HFD, an insulin tolerance test was administered in WT (solid line) and *eNos Tg* (dotted line) mice. Results were expressed as percent drop of the basal glucose after intraperitoneal injection of insulin. *E* and *F*: Liver lysates were analyzed for IκB-α phosphorylation by Western blot and IL-6 mRNA expression by RT-PCR. *G* and *H*: Hepatic insulin signaling was assessed after intraperitoneal injection of insulin. Liver protein lysates were analyzed for p-IRS2, IRS2, Akt serine phosphorylation (p-Akt), and Akt levels by ELISA. *I*: Hepatic TG content. *J*: Liver lysates were analyzed for VASP serine 239 phosphorylation. *$P < 0.05$ (n = 4–5 per group). ins, insulin; veh, vehicle.

obesity, and, as expected, liver TG content increased by greater than twofold after 14 weeks of HFD feeding in WT mice. Remarkably, this effect of obesity to induce hepatic steatosis was completely absent in *eNos Tg* mice (Fig. 1*I*). Collectively, these results suggest that the effect of HFD-induced obesity to reduce hepatic NO signaling is required for the development of hepatic inflammation, steatosis, and hepatic insulin resistance.

Our previous studies demonstrated that HFD feeding reduces hepatic VASP serine 239 phosphorylation as well as NO content (19), and deficiency of either VASP or eNOS mimic the effect of HFD feeding to induce hepatic NF-κB activation and insulin resistance (19). We therefore sought to determine whether the effect of eNOS overexpression to ameliorate obesity-associated hepatic inflammation and hepatic insulin resistance (Fig. 1*E* and *F*) also reverses the effect of HFD feeding to reduce VASP phosphorylation in liver. Whole-liver lysates from WT and *eNos Tg* mice fed an HFD for 8 weeks were analyzed by Western blot for serine 239 VASP phosphorylation (Fig. 1*I*). Whereas WT mice exhibited the expected decrease of hepatic serine 239 VASP phosphorylation content in WT mice, this effect was not observed in *eNos Tg* mice.

Based on these findings, and because the polarization of Kupffer cells toward an inflammatory M1 and away from an anti-inflammatory M2 phenotype is implicated in obesity-induced hepatic inflammation and hepatic insulin resistance (13,35), we next wished to determine *1*) whether the protective effect of eNOS is mediated by increased VASP signaling during obesity-associated hepatic inflammation and *2*) whether Kupffer cells are targets for the

anti-inflammatory effect of increased hepatic endothelial NO → VASP signaling.

Effect of Increased Hepatic eNOS Expression on Kupffer Cell M1 and M2 Polarization

To determine whether the effect of HFD feeding induce M1 activation of Kupffer cells is dependent on reduced endothelial NO → VASP signaling, we measured M1 and M2 markers in Kupffer cells isolated from the liver of WT and *eNos Tg* mice fed either an HFD or an LFD for 8 weeks. As expected, HFD feeding induced M1 markers (tumor necrosis factor [TNF], IL-6) in the liver of WT mice compared with LFD-fed controls, and this effect was blunted in *eNos Tg* mice (Fig. 2*A*). To determine whether acquisition of the M2 phenotype in Kupffer cells is enhanced by increased endothelial NO signaling in vivo, groups of mice from each genotype were injected with IL-4 (3 mg/day i.p. for 3 days) prior to Kupffer cell harvest. In WT mice, HFD feeding was associated with reduced expression of M2 markers (Arg1, Ym1, and peroxisome proliferator–activated receptor γ coactivator-1β [PGC-1β]) compared with Kupffer cells from LFD-fed controls, but this effect of HFD feeding was not observed in the liver of *eNos Tg* mice (Fig. 2*B*). Reduced hepatic NO content is therefore required for the effect of obesity to polarize Kupffer cells toward the M1 and away from the M2 phenotype.

Hematopoietic VASP Deficiency Mimics Obesity-Associated Hepatic Inflammation, Insulin Resistance, and Kupffer Cell Activation

Based on our previous finding that whole-body VASP knockout produces a predisposition to liver inflammation and proinflammatory Kupffer cell activation during HFD feeding (19), we next sought to determine whether deficiency of VASP specifically within cells of bone marrow lineage (including Kupffer cells) is sufficient to mimic these hepatic effects of whole-body VASP deficiency. To accomplish this goal, we transplanted either WT or VASP-deficient bone marrow into sublethally irradiated WT mice (11,36). After a 4-week recovery period, engraftment was confirmed by Western blot analysis showing that the absence of VASP protein from BMDMs obtained from WT mice reconstituted VASP-deficient bone marrow (VASP KO-BMT mice) (Fig. 3*A*). Mice were subsequently placed on an LFD for 4 weeks, a diet that does not induce hepatic inflammation or insulin resistance in normal mice (21).

Body weights were similar in VASP KO-BMT mice and WT mice with WT bone marrow (WT-BMT mice) (Fig. 3*B*). Despite consuming an LFD, reconstitution of WT mice with VASP-deficient bone marrow also resulted in hepatic inflammation and hepatic insulin resistance resembling that induced by HFD feeding in normal mice (Fig. 3*C* and *D*). These findings indicate that limiting the deficiency of VASP to bone marrow-derived cells is sufficient to mimic the hepatic inflammation and insulin resistance phenotype of mice with global VASP deficiency.

Since Kupffer cells (like other macrophages) are derived from bone marrow whereas most other hepatic cell types are not, they are expected to lack VASP in VASP KO-BMT mice, but not in WT-BMT mice. We therefore asked whether Kupffer cell polarization is affected by reduced VASP signaling in bone marrow–derived cells by comparing M1 markers from Kupffer cells isolated from VASP KO-BMT with those from WT-BMT mice. Importantly, genes associated with M1 activation were expressed at a much higher level in Kupffer cells derived from the former group (Fig. 3*E*). Genetic deletion of VASP in bone marrow–derived cells, therefore, is sufficient not only to cause liver inflammation and insulin resistance, but to trigger Kupffer cell M1 inflammatory activation as well.

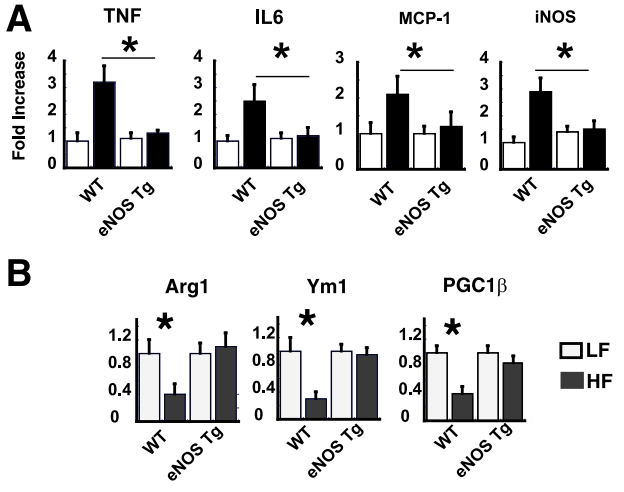

Figure 2—Effect of increased endothelial NO levels on Kupffer cell polarization. *A* and *B*: Eight-week-old WT and *eNos Tg* mice were maintained on either an LFD (LF) or HFD (HF) for 8 weeks; and, for the stimulation of the expression of M2 marker genes, study mice received daily intraperitoneal injection of IL-4 complexes for the last 3 days of the diet. *A*: Expression of M1 marker genes from isolated Kupffer cells, as measured by RT-PCR (n = 10 per group). *B*: M2 marker genes from isolated Kupffer cells by RT-PCR (n = 5 per group). *P < 0.05. iNOS, inducible NO synthase.

Effect of Endothelial NO Signaling on M1 and M2 Polarization in Cultured Macrophages

To further test the hypothesis that endothelial NO signaling polarizes macrophages away from the M1 and toward the anti-inflammatory M2 phenotype, we used a coculture system combining BAECs (as a source of endothelial NO) with BMDMs. As a specificity control, the BAECs used for this study were either intact or had a reduced capacity to generate NO (by prior incubation with scrambled control siRNA or eNOS siRNA, respectively). As expected, eNOS expression was markedly reduced in BAECs receiving eNOS versus scrambled siRNA (Fig. 4*A*), and ESR (37,38) measurements demonstrated a proportionate reduction of NO content in the former (Fig. 4*B*). To determine whether decreased endothelial NO enhances M1 activation of BMDMs, cells were stimulated with LPS and IFN-γ. Compared with BMDMs cocultured with control endothelial cells, the induction of M1

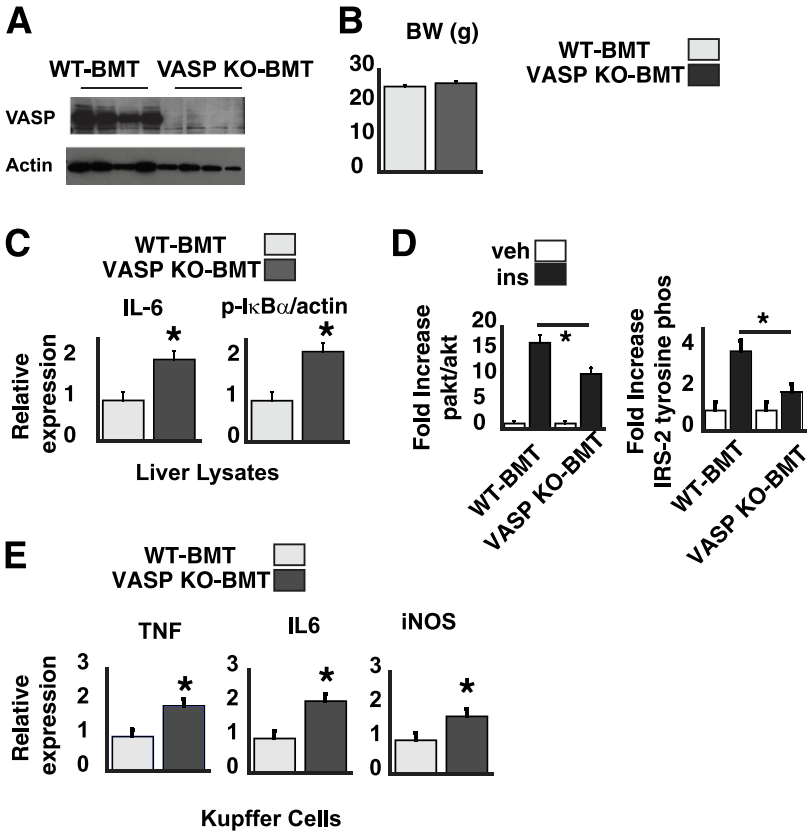

Figure 3—Effect of VASP deficiency in immune cells on hepatic inflammation and insulin resistance. C57BL/6 WT and *Vasp*$^{-/-}$ mice were irradiated, and their bone marrow was reconstituted with either WT or VASP-deficient bone marrow, creating the following two groups of chimeric mice: WT-BMT (WT bone marrow transplanted into WT mice) and VASP KO-BMT (*Vasp*$^{-/-}$ bone marrow transplanted into WT mice). After recovery from the bone marrow transplantation, the chimeras were placed on an LFD for 4 weeks. *A*: VASP and actin Western blots from BMDM lysates. *B*: Body weight (BW) (g). *C*: Liver lysates were analyzed for IκB-α phosphorylation (phos) by Western blot and for IL-6 mRNA expression by RT-PCR. *D*: Vehicle or insulin (0.6 units/g body wt i.p.) was injected, and fold increases of pAKT and p-IRS2 in liver lysates were measured by ELISA. *E*: M1 markers were measured by RT-PCR in isolated Kupffer cells from WT-BMT and VASP KO-BMT mice. **P* < 0.05, *n* = 5 for each group. iNOS, inducible NO synthase; ins, insulin; veh, vehicle.

markers was enhanced in BMDMs cocultured with eNOS-depleted BAECs (Fig. 4*C*). The increase of lactate levels, a marker of a metabolic shift toward the anaerobic glycolytic pathway, which is characteristic of the M1 activation phenotype (39,40), in response to LPS and IFN-γ treatment was also enhanced in BMDMs cocultured with eNOS-depleted versus eNOS-replete BAECs (Fig. 4*D*).

To determine whether decreased endothelial NO signaling has the opposite effect on macrophage M2 activation, the coculture study was repeated except that BMDMs were incubated with IL-4, rather than LPS and IFN-γ. As expected, IL-4 treatment increased the expression of M2 markers Arg1 and Ym1 mRNA in BMDMs cocultured with eNOS-replete BAECs, and this effect was blunted in BMDMs cocultured with eNOS-deficient BAECs (Fig. 4*E*). These findings offer direct support for the hypothesis that endothelial NO limits M1 and favors M2 macrophage polarization.

To confirm that increased endothelial NO signaling polarizes macrophages away from the M1 and toward the M2 phenotype, BMDMs from C57BL/6 mice were pretreated with DETA-NO, a NO donor, and M1 and M2 activation markers were measured after stimulation with LPS plus either IFN-γ or IL-4. Compared with vehicle-treated BMDMs, DETA-NO treatment reduced levels of mRNA encoding M1 markers (TNF, IL-6) while raising the expression of M2 markers Arg1 and Ym1 (Fig. 4*F*). Therefore, increased NO levels attenuate the inflammatory M1 and increase anti-inflammatory M2 polarization irrespective of whether endothelial cells are the NO source.

VASP Deficiency Reduces M2 Polarization of Macrophages

To determine whether VASP regulates macrophage polarization in vivo, we next analyzed BMDM from WT and *Vasp*$^{-/-}$ mice for anti-inflammatory M2 gene expression after stimulation with IL-4. Notably, IL-4–mediated induction of M2 markers (Arg1 protein and mRNA encoding *Ym1*, *Arg1*, and mannose receptor) was dramatically reduced in BMDMs from VASP-deficient mice (Fig. 5*A* and *B*). Because IL-4–mediated M2 polarization is also characterized by increased macrophage fatty acid uptake and oxidation (13,33), we also measured the expression levels

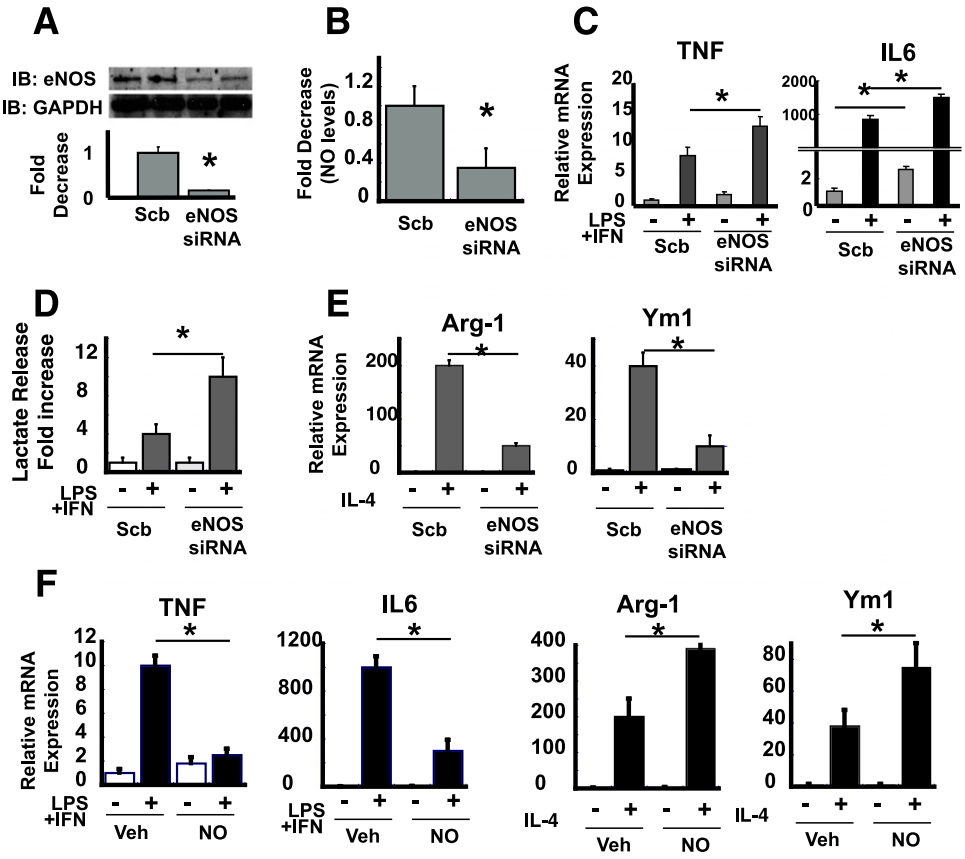

Figure 4—Effect of increased or decreased levels of NO on macrophage polarization. BMDMs were cocultured with BAECs transfected with either control (Scb) siRNA or eNOS siRNA and cultured for 48 h. *A*: Representative Western blot showing eNOS siRNA-mediated reduction of eNOS protein expression in BAECs. *B*: NO content as measured by ESR. *C*: BMDMs were stimulated with LPS (5 ng/mL) and IFN-γ (12 ng/mL) for 24 h and then were analyzed for TNF-α, IL-6, and iNOS mRNA expression ($n = 4$). *D*: Lactate levels in media after stimulation with LPS (5 ng/mL) and IFN-γ (12 ng/mL) ($n = 4$). *E*: Arg1 and Ym1 mRNA expression in BMDMs stimulated with IL-4 (10 ng/mL for 48 h) ($n = 4$). *F*: BMDMs from WT mice were stimulated with LPS (5 ng/mL) plus IFN-γ (12 ng/mL) for 24 h or IL-4 for 48 h in the presence or absence of DETA-NO (10 μmol/L for 4 h). TNF-α, IL-6, Arg1, and Ym1 mRNA expression as measured by RT-PCR ($n = 4$). *$P < 0.05$. veh, vehicle.

of genes involved in fatty acid oxidation from these cells. Consistent with a global decline in M2 activation markers, levels of mRNA encoding PGC-1β, peroxisome proliferator–activated receptor-γ (PPARγ), carnitine palmitoyl-transferase 1, and peroxisomal acyl-coenzyme A oxidase 1 were markedly reduced in BMDMs from *Vasp*$^{-/-}$ mice after incubation with IL-4 (Fig. 5*C*).

As the biological effect of IL-4 receptor stimulation involves the activation of the IL-4/STAT6 pathway (41,42), we evaluated whether signaling via this pathway is disrupted in BMDMs from *Vasp*$^{-/-}$ mice. Consistent with this hypothesis, the treatment of WT BMDMs with IL-4 increased STAT6 tyrosine phosphorylation (Fig. 5*D*), but this effect again was attenuated in VASP-deficient macrophages. Collectively, these results suggest that VASP is required for macrophage M2 activation in response to IL-4.

VASP Signaling Regulates M1 Polarization of Macrophages

Comparing proinflammatory gene expression in control versus VASP-deficient BMDMs after stimulation with LPS and IFN-γ, rather than IL-4, revealed a potent effect of VASP deficiency to enhance the induction of M1 markers (Fig. 6*A*), and lactate production by VASP-deficient BMDMs was also greater than that by control BMDMs (Fig. 6*A*). To determine whether increased VASP signaling has the opposite effect, we used RAW cells, a macrophage cell line. Consistent with our previous data (19), we observed that, compared with RAW cells transduced with empty vector, virally mediated overexpression of VASP in RAW cells attenuated LPS/IFN-γ–induced M1 gene expression (Fig. 6*B*), and this effect was associated with reduced lactate levels (Fig. 6*B*). These data collectively suggest that intact VASP signaling is both necessary and sufficient to inhibit LPS/IFN-γ–induced macrophage M1 activation.

DISCUSSION

Macrophages undergo phenotypic changes in response to various environmental signals that can dramatically alter their function. The clinical relevance of this phenomenon stems in part from accumulating evidence that proinflammatory M1 polarization of macrophages contributes

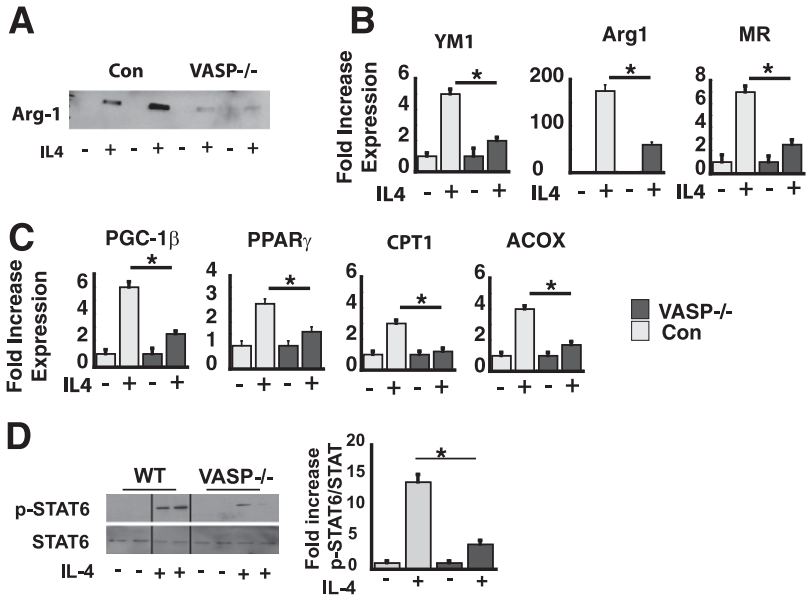

Figure 5—Effect of VASP deficiency on macrophage M2 polarization. BMDMs from WT and *Vasp*$^{-/-}$ mice were stimulated with IL-4 (10 ng/mL for 48 h). *A*: Representative Western blot showing Arg1 protein expression (n = 4). *B*: M2 marker gene [Ym1, Arg1, and mannose receptor (MR)] expression as measured by RT-PCR. *C*: Expression of genes (PGC-1β, PPARγ, CPT1, ACOX) involved in fatty acid metabolism by RT-PCR. *D*: Phospho-STAT6 protein expression as measured by Western blot. Vertical division lines have been inserted to mark sites where the picture file has been cut and repositioned to remove lanes from loading artifact; the remaining lanes were on the same gel run at the same time. *P < 0.05.

to metabolic impairment that is associated with obesity and diabetes (2,43). Thus, the deletion of M1 (classically activated) tissue macrophages normalizes sensitivity to insulin in obese mice (44,45), while, conversely, the reduction of M2 (alternatively activated) macrophages predisposes lean mice to the development of insulin resistance (13), implying a critical role for M2 polarization of macrophages in metabolic homeostasis. The current work suggests that in Kupffer cells, endothelial NO signaling maintains M2 polarization, whereas the effect of HFD feeding to reduce hepatic NO signaling reduces M2 and favors M1 polarization of these cells. This conclusion offers a feasible explanation for the findings that deficient NO signaling induces hepatic insulin resistance (19,46,47), whereas HFD-induced hepatic insulin resistance is blocked by preventing the accompanying decline of hepatic endothelial

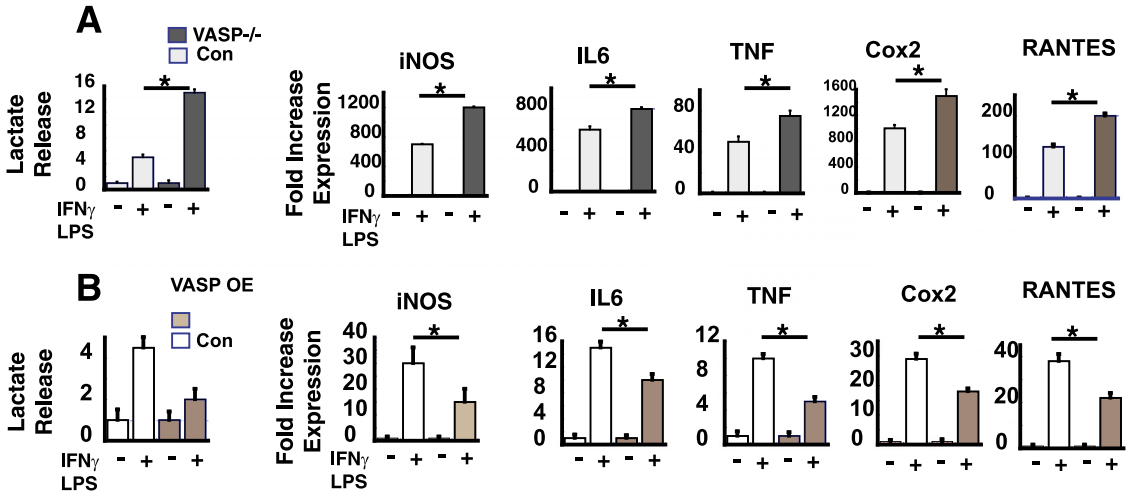

Figure 6—Effect of VASP signaling on macrophage M1 polarization. *A*: BMDMs from WT and *Vasp*$^{-/-}$ mice were stimulated with LPS (5 ng/mL) and IFN-γ (12 ng/mL) for 1 h. M1 markers, as measured by RT-PCR (n = 4). Lactate levels in BMDM media (n = 4 per group). *B*: RAW cells were transduced with VASP (VASP-OE) or control (Con) vector. Expression of M1 marker genes by RT-PCR (n = 5). Lactate levels in RAW cell media (n = 4). *P < 0.05. Cox2, cyclooxygenase 2; iNOS, inducible NO synthase; RANTES, regulated on activation normal T cell expressed and secreted.

NO content (Fig. 1). In the current work, we report both in vitro and in vivo data suggesting that NO reduces M1 polarization and increases M2, whereas the absence of NO has the opposite effect (Figs. 2 and 4). Moreover, we extend prior evidence of an important role for VASP (19,20,48) as a downstream mediator of the effects of NO to prevent obesity-associated hepatic insulin resistance via effects that can be localized to macrophages (Fig. 3). Specifically, we report that macrophage VASP signaling mediates the effect of endothelial NO to promote macrophage M2 polarization. Together, these findings provide compelling evidence that under physiological conditions, the maintenance of macrophage M2 polarization depends upon sufficient NO → VASP signaling.

Advances in our understanding of the complex interactions between immune and metabolic cell types raise interesting possibilities regarding the future treatment of obesity-associated metabolic impairment. In this regard, it is noteworthy that medications that increase NO signaling medications, such as the phosphodiesterase-5 (PDE5) inhibitor sildenafil, are already in wide use. Our laboratory and others have shown that, in mice, sildenafil increases endothelial NO signaling (by inhibiting degradation of cGMP), reduces several markers of insulin resistance (49–51) while restoring hepatic insulin signaling (19), prevents Kupffer cell M1 activation during HFD feeding, and reduces hepatic TG content. Whether PDE5 inhibitors can be of similar benefit in humans remains to be investigated, but several possibilities exist beyond PDE5 inhibition. For example, a number of NO donor compounds are currently available (52,53) that are known to increase NO bioavailability and thereby exert anti-inflammatory effects. Sodium nitrite/nitrate (NO_{2-}, NO_{3-}) is a potential NO reservoir that also appears to protect against diabetes in a model of obesity induced by HFD feeding (54). It will be of interest to determine whether a NO-based therapeutic intervention directed at macrophage polarization offers an additional therapeutic strategy for attenuating the development of insulin resistance and diabetes.

Signal transduction induced by eNOS-derived NO involves cGMP and PKG, which in turn regulates the activity of a host of downstream targets. Among these is VASP, which is phosphorylated by PKG on a specific serine residue (Ser 239). Our previous studies (19) have implicated VASP as a key mediator of the anti-inflammatory effects of endothelial NO in both adipose tissue and liver, including inflammatory activation of Kupffer cells. A key goal of the current studies was to delineate whether NO → VASP signaling plays a physiological role in macrophage polarization. Consistent with this hypothesis, we found that VASP deficiency induces M1 while reducing M2 macrophage activation both in vivo and in cultured cells, whereas VASP overexpression is associated with the opposite outcome (attenuation of LPS- and IFN-γ–induced expression of inflammatory markers and lactate release). VASP deficiency and overexpression, therefore, appear to reproduce the effects on macrophages of reduced and increased endothelial NO signaling, respectively. This finding implicates VASP as a key downstream mediator of endothelial NO signaling in the control of macrophage polarization.

A key question raised by these findings is whether VASP deficiency, specifically in the macrophage compartment, is sufficient to explain the hepatic inflammation and hepatic insulin resistance that is characteristic of mice with whole-body deficiency of either eNOS or VASP. If so, the phenotype of hepatic inflammation and insulin resistance seen with whole-body VASP deficiency should be present in mice lacking VASP only in bone marrow–derived cells as well. We therefore performed bone marrow transplantation experiments to test this hypothesis. When we compared the expression of inflammatory markers and insulin signaling in livers of WT mice transplanted with WT bone marrow (WT-BMT mice) to that of WT mice transplanted with VASP-deficient bone marrow (VASP KO-BMT mice), the latter group exhibited the pattern of hepatic inflammation and insulin resistance seen with HFD feeding, even though the mice were maintained on an LFD. Moreover, mice in the VASP KO-BMT group also exhibited inflammatory activation of Kupffer cells, suggesting that VASP signaling in macrophages plays a physiological role to protect against hepatic inflammation and insulin signaling. Consistent with this interpretation, we also observed that the hepatic manifestations of long-term HFD feeding are abrogated by the overexpression of endothelial eNOS. These observations support a model in which the effect of HFD feeding to reduce hepatic NO → VASP signaling is linked to hepatic inflammation and metabolic impairment via M1 activation of Kupffer cells.

The current work does not specifically address the effect of eNOS/VASP on adipose tissue inflammation and adipose tissue macrophage activation. It is possible that the activation of adipose inflammatory pathways could contribute to the hepatic and Kupffer cell phenotype observed in the current study, since the deletion of Vasp in the bone marrow–derived cell line also affects adipose tissue macrophages, which could indirectly affect hepatic insulin resistance.

At the transcriptional level, numerous factors have been identified as mediators of macrophage polarization. Among those factors implicated in the M1 macrophage phenotype are NF-κB, activated protein-1, STAT-1, C/EBPβ, PU.1, Krüppel-like factor (KLF) 6, and IFN regulatory factor (6,55,56), whereas STAT6, IFN regulatory factor-4, KLF4, KLF6, and PPARγ are implicated in M2 macrophage polarization (7,43,56–59). Based on our current findings, we propose that the endothelial NO → VASP pathway be added to the list of signal transduction mechanisms that participate in macrophage polarization, and that future studies are warranted to delineate the molecular effectors that link VASP signaling to the M2 macrophage phenotype. One possibility involves the known

effect of NO to alter gene expression by epigenetic regulation through histone modification (60,61), and recent studies implicate this type of mechanism in the control of macrophage polarization (62,63). In addition, the activation of AMPK is reported to prevent proinflammatory cytokine production by macrophages (64), whereas the AMPK β1 subunit loss enhances adipose tissue macrophage inflammation and liver insulin resistance during HFD feeding (65). Since VASP enhances hepatic fatty acid oxidation by activating AMPK (48), and since AMPK can affect macrophage polarization, a role for AMPK in the effect of NO/VASP signaling on macrophage polarization can be considered, and studies to test this hypothesis are warranted.

In summary, we provide the first direct evidence that the effect of endothelial NO to activate VASP signaling in macrophages exerts anti-inflammatory effects by promoting M2 macrophage polarization, and that the effect of HFD feeding to reduce signaling via this pathway causes M1 activation of Kupffer cells that, in turn, contributes to the associated hepatic inflammation and hepatic insulin resistance. These findings identify the macrophage endothelial NO → VASP signaling pathway as a novel therapeutic target for the treatment of metabolic disorders, including obesity and diabetes.

Funding. This study was supported by grants from the National Institutes of Health (NIH) by National Institute of Diabetes and Digestive and Kidney Diseases (NIDDK) grants DK-068384, DK-083042, DK-090320, and DK-101997 (M.W.S.) and DK-073878 (F.K.); University of Washington Nutrition Obesity Research Center grant DK-035816; University of Washington Diabetes Research Center Cell Function Analysis Core grant DK-17047 (I.R.S.); NIH Cardiovascular Postdoctoral Training grants T32-HL-07828 (A.M.C.), HL-52459 (A.W.C.), and DK-083310; NIDDK Diabetic Complications Consortium Pilot and Feasibility grant DK-076169 (K.B.); and a grant from the John L. Locke Jr. Charitable Trust and from the Kenneth H. Cooper, M.D. Endowed Professorship in Preventive Cardiology (F.K.).

Duality of Interest. No potential conflicts of interest relevant to this article were reported.

Author Contributions. W.J.L. and S.T. designed and performed the experiments, provided data analysis, wrote the manuscript, contributed to discussion, and reviewed and edited the manuscript. A.M.C., N.R.-D., N.F.W., P.H., and C.L.W. designed and performed the experiments and provided data analysis. A.W.C., I.R.S., and K.B. designed the experiments, provided data analysis, and wrote the manuscript. M.W.S. and F.K. designed the experiments, provided data analysis, wrote the manuscript, and reviewed and edited the manuscript. W.J.L., S.T., and F.K. are the guarantors of this work and, as such, had full access to all the data in the study and take responsibility for the integrity of the data and the accuracy of the data analysis.

References

1. Odegaard JI, Chawla A. Pleiotropic actions of insulin resistance and inflammation in metabolic homeostasis. Science 2013;339:172–177
2. Gordon S, Taylor PR. Monocyte and macrophage heterogeneity. Nat Rev Immunol 2005;5:953–964
3. Murray PJ, Wynn TA. Protective and pathogenic functions of macrophage subsets. Nat Rev Immunol 2011;11:723–737
4. Biswas SK, Mantovani A. Macrophage plasticity and interaction with lymphocyte subsets: cancer as a paradigm. Nat Immunol 2010;11:889–896
5. Sica A, Mantovani A. Macrophage plasticity and polarization: in vivo veritas. J Clin Invest 2012;122:787–795
6. Olefsky JM, Glass CK. Macrophages, inflammation, and insulin resistance. Annu Rev Physiol 2010;72:219–246
7. Odegaard JI, Chawla A. Alternative macrophage activation and metabolism. Annu Rev Pathol 2011;6:275–297
8. Chawla A, Nguyen KD, Goh YP. Macrophage-mediated inflammation in metabolic disease. Nat Rev Immunol 2011;11:738–749
9. Hotamisligil GS. Inflammation and metabolic disorders. Nature 2006;444:860–867
10. Shoelson SE, Lee J, Goldfine AB. Inflammation and insulin resistance. J Clin Invest 2006;116:1793–1801
11. Odegaard JI, Ricardo-Gonzalez RR, Red Eagle A, et al. Alternative M2 activation of Kupffer cells by PPARdelta ameliorates obesity-induced insulin resistance. Cell Metab 2008;7:496–507
12. Bouloumié A, Curat CA, Sengenès C, Lolmède K, Miranville A, Busse R. Role of macrophage tissue infiltration in metabolic diseases. Curr Opin Clin Nutr Metab Care 2005;8:347–354
13. Odegaard JI, Ricardo-Gonzalez RR, Goforth MH, et al. Macrophage-specific PPARgamma controls alternative activation and improves insulin resistance. Nature 2007;447:1116–1120
14. Odegaard JI, Chawla A. Mechanisms of macrophage activation in obesity-induced insulin resistance. Nat Clin Pract Endocrinol Metab 2008;4:619–626
15. Laroux FS, Lefer DJ, Kawachi S, et al. Role of nitric oxide in the regulation of acute and chronic inflammation. Antioxid Redox Signal 2000;2:391–396
16. Huang PL. eNOS, metabolic syndrome and cardiovascular disease. Trends Endocrinol Metab 2009;20:295–302
17. Blume C, Benz PM, Walter U, Ha J, Kemp BE, Renné T. AMP-activated protein kinase impairs endothelial actin cytoskeleton assembly by phosphorylating vasodilator-stimulated phosphoprotein. J Biol Chem 2007;282:4601–4612
18. Trichet L, Sykes C, Plastino J. Relaxing the actin cytoskeleton for adhesion and movement with Ena/VASP. J Cell Biol 2008;181:19–25
19. Tateya S, Rizzo NO, Handa P, et al. Endothelial NO/cGMP/VASP signaling attenuates Kupffer cell activation and hepatic insulin resistance induced by high-fat feeding. Diabetes 2011;60:2792–2801
20. Handa P, Tateya S, Rizzo NO, et al. Reduced vascular nitric oxide-cGMP signaling contributes to adipose tissue inflammation during high-fat feeding. Arterioscler Thromb Vasc Biol 2011;31:2827–2835
21. Kim F, Pham M, Maloney E, et al. Vascular inflammation, insulin resistance, and reduced nitric oxide production precede the onset of peripheral insulin resistance. Arterioscler Thromb Vasc Biol 2008;28:1982–1988
22. Ohashi Y, Kawashima S, Hirata Ki, et al. Hypotension and reduced nitric oxide-elicited vasorelaxation in transgenic mice overexpressing endothelial nitric oxide synthase. J Clin Invest 1998;102:2061–2071
23. Chen L, Daum G, Chitaley K, et al. Vasodilator-stimulated phosphoprotein regulates proliferation and growth inhibition by nitric oxide in vascular smooth muscle cells. Arterioscler Thromb Vasc Biol 2004;24:1403–1408
24. Meininger CJ, Marinos RS, Hatakeyama K, et al. Impaired nitric oxide production in coronary endothelial cells of the spontaneously diabetic BB rat is due to tetrahydrobiopterin deficiency. Biochem J 2000;349:353–356
25. Cai S, Khoo J, Mussa S, Alp NJ, Channon KM. Endothelial nitric oxide synthase dysfunction in diabetic mice: importance of tetrahydrobiopterin in eNOS dimerisation. Diabetologia 2005;48:1933–1940
26. Alp NJ, Mussa S, Khoo J, et al. Tetrahydrobiopterin-dependent preservation of nitric oxide-mediated endothelial function in diabetes by targeted transgenic GTP-cyclohydrolase I overexpression. J Clin Invest 2003;112:725–735
27. Elrod JW, Duranski MR, Langston W, et al. eNOS gene therapy exacerbates hepatic ischemia-reperfusion injury in diabetes: a role for eNOS uncoupling. Circ Res 2006;99:78–85
28. Jenkins SJ, Ruckerl D, Cook PC, et al. Local macrophage proliferation, rather than recruitment from the blood, is a signature of TH2 inflammation. Science 2011;332:1284–1288

29. Kim F, Pham M, Luttrell I, et al. Toll-like receptor-4 mediates vascular inflammation and insulin resistance in diet-induced obesity. Circ Res 2007;100:1589–1596
30. Kim F, Tysseling KA, Rice J, et al. Free fatty acid impairment of nitric oxide production in endothelial cells is mediated by IKKbeta. Arterioscler Thromb Vasc Biol 2005;25:989–994
31. Alp NJ, McAteer MA, Khoo J, Choudhury RP, Channon KM. Increased endothelial tetrahydrobiopterin synthesis by targeted transgenic GTP-cyclohydrolase I overexpression reduces endothelial dysfunction and atherosclerosis in ApoE-knockout mice. Arterioscler Thromb Vasc Biol 2004;24:445–450
32. Kanda H, Tateya S, Tamori Y, et al. MCP-1 contributes to macrophage infiltration into adipose tissue, insulin resistance, and hepatic steatosis in obesity. J Clin Invest 2006;116:1494–1505
33. Vats D, Mukundan L, Odegaard JI, et al. Oxidative metabolism and PGC-1beta attenuate macrophage-mediated inflammation. Cell Metab 2006;4:13–24
34. Muniyappa R, Lee S, Chen H, Quon MJ. Current approaches for assessing insulin sensitivity and resistance in vivo: advantages, limitations, and appropriate usage. Am J Physiol Endocrinol Metab 2008;294:E15–E26
35. Obstfeld AE, Sugaru E, Thearle M, et al. C-C chemokine receptor 2 (CCR2) regulates the hepatic recruitment of myeloid cells that promote obesity-induced hepatic steatosis. Diabetes 2010;59:916–925
36. Weisberg SP, McCann D, Desai M, Rosenbaum M, Leibel RL, Ferrante AW Jr. Obesity is associated with macrophage accumulation in adipose tissue. J Clin Invest 2003;112:1796–1808
37. Duranski MR, Elrod JW, Calvert JW, Bryan NS, Feelisch M, Lefer DJ. Genetic overexpression of eNOS attenuates hepatic ischemia-reperfusion injury. Am J Physiol Heart Circ Physiol 2006;291:H2980–H2986
38. Khoo JP, Alp NJ, Bendall JK, et al. EPR quantification of vascular nitric oxide production in genetically modified mouse models. Nitric Oxide 2004;10:156–161
39. Peyssonnaux C, Datta V, Cramer T, et al. HIF-1alpha expression regulates the bactericidal capacity of phagocytes. J Clin Invest 2005;115:1806–1815
40. Rodríguez-Prados JC, Través PG, Cuenca J, et al. Substrate fate in activated macrophages: a comparison between innate, classic, and alternative activation. J Immunol 2010;185:605–614
41. Ricardo-Gonzalez RR, Red Eagle A, Odegaard JI, et al. IL-4/STAT6 immune axis regulates peripheral nutrient metabolism and insulin sensitivity. Proc Natl Acad Sci U S A 2010;107:22617–22622
42. Wurster AL, Tanaka T, Grusby MJ. The biology of Stat4 and Stat6. Oncogene 2000;19:2577–2584
43. Charo IF. Macrophage polarization and insulin resistance: PPARgamma in control. Cell Metab 2007;6:96–98
44. Lumeng CN, Bodzin JL, Saltiel AR. Obesity induces a phenotypic switch in adipose tissue macrophage polarization. J Clin Invest 2007;117:175–184
45. Patsouris D, Li PP, Thapar D, Chapman J, Olefsky JM, Neels JG. Ablation of CD11c-positive cells normalizes insulin sensitivity in obese insulin resistant animals. Cell Metab 2008;8:301–309
46. Shankar RR, Wu Y, Shen HQ, Zhu JS, Baron AD. Mice with gene disruption of both endothelial and neuronal nitric oxide synthase exhibit insulin resistance. Diabetes 2000;49:684–687
47. Duplain H, Burcelin R, Sartori C, et al. Insulin resistance, hyperlipidemia, and hypertension in mice lacking endothelial nitric oxide synthase. Circulation 2001;104:342–345
48. Tateya S, Rizzo-De Leon N, Handa P, et al. VASP increases hepatic fatty acid oxidation by activating AMPK in mice. Diabetes 2013;62:1913–1922
49. Ayala JE, Bracy DP, Julien BM, Rottman JN, Fueger PT, Wasserman DH. Chronic treatment with sildenafil improves energy balance and insulin action in high fat-fed conscious mice. Diabetes 2007;56:1025–1033
50. Rizzo NO, Maloney E, Pham M, et al. Reduced NO-cGMP signaling contributes to vascular inflammation and insulin resistance induced by high-fat feeding. Arterioscler Thromb Vasc Biol 2010;30:758–765
51. Behr-Roussel D, Oudot A, Caisey S, et al. Daily treatment with sildenafil reverses endothelial dysfunction and oxidative stress in an animal model of insulin resistance. Eur Urol 2008;53:1272–1280
52. Carpenter AW, Schoenfisch MH. Nitric oxide release: part II. Therapeutic applications. Chem Soc Rev 2012;41:3742–3752
53. Megson IL, Webb DJ. Nitric oxide donor drugs: current status and future trends. Expert Opin Investig Drugs 2002;11:587–601
54. Carlström M, Larsen FJ, Nyström T, et al. Dietary inorganic nitrate reverses features of metabolic syndrome in endothelial nitric oxide synthase-deficient mice. Proc Natl Acad Sci U S A 2010;107:17716–17720
55. Takeuchi O, Akira S. Pattern recognition receptors and inflammation. Cell 2010;140:805–820
56. Date D, Das R, Narla G, Simon DI, Jain MK, Mahabeleshwar GH. Kruppel-like transcription factor 6 regulates inflammatory macrophage polarization. J Biol Chem 2014;289:10318–10329
57. Liao X, Sharma N, Kapadia F, et al. Krüppel-like factor 4 regulates macrophage polarization. J Clin Invest 2011;121:2736–2749
58. Szanto A, Balint BL, Nagy ZS, et al. STAT6 transcription factor is a facilitator of the nuclear receptor PPARγ-regulated gene expression in macrophages and dendritic cells. Immunity 2010;33:699–712
59. Gordon S. Do macrophage innate immune receptors enhance atherogenesis? Dev Cell 2003;5:666–668
60. Hickok JR, Vasudevan D, Antholine WE, Thomas DD. Nitric oxide modifies global histone methylation by inhibiting Jumonji C domain-containing demethylases. J Biol Chem 2013;288:16004–16015
61. Li Q, Sarna SK. Nitric oxide modifies chromatin to suppress ICAM-1 expression during colonic inflammation. Am J Physiol Gastrointest Liver Physiol 2012;303:G103–G110
62. Medzhitov R, Horng T. Transcriptional control of the inflammatory response. Nat Rev Immunol 2009;9:692–703
63. De Santa F, Totaro MG, Prosperini E, Notarbartolo S, Testa G, Natoli G. The histone H3 lysine-27 demethylase Jmjd3 links inflammation to inhibition of polycomb-mediated gene silencing. Cell 2007;130:1083–1094
64. Kohlstedt K, Trouvain C, Namgaladze D, Fleming I. Adipocyte-derived lipids increase angiotensin-converting enzyme (ACE) expression and modulate macrophage phenotype. Basic Res Cardiol 2011;106:205–215
65. Galic S, Fullerton MD, Schertzer JD, et al. Hematopoietic AMPK β1 reduces mouse adipose tissue macrophage inflammation and insulin resistance in obesity. J Clin Invest 2011;121:4903–4915